

SLIDING MODE CONTROLLER FOR THE BOOST INVERTER

Ramón Cáceres
 Universidad de los Andes
 Facultad de Ingeniería
 Dpto. de Electrónica
 Mérida - Edo. Mérida - Venezuela.
 E-mail: rcaceres@ing.ula.ve
 ramon@inep.ufsc.br
 Tel: 58-74-402907
 Fax: 58-74-402947

Ivo Barbi
 Federal University of Santa Catarina.
 Dpto. Electrical Engineering
 Power Electronics Institute (INEP)
 P.O.Box: 5119 (88040-970)
 Florianópolis - SC - Brazil
 E-mail: ivo@inep.ufsc.br
 Tel: 55-48-231-9204
 Fax: 55-48-234-5422

Abstract: The Sliding mode control theory is applied to a sinusoidal output voltage boost inverter with linear load. The boost inverter is intended to be used in UPS design, whenever an AC voltage larger than the DC link voltage is needed, with no need of a second power conversion stage. Operation, control strategy, simulation and experimental results are included in this paper.

INTRODUCTION

Static and dynamic characteristics of boost DC - AC converter have been discussed in the literature [1], [2], where tools for analysis, modeling and design are available.

The boost DC - AC converter, referred to as boost inverter, features an excellent property: it naturally generates an output AC voltage lower or larger than the input DC voltage, depending on the duty cycle. This property is not found in the classical voltage source inverter which produces an AC instantaneous output voltage always lower than the input DC voltage.

For the purpose of optimizing the boost inverter dynamics, while ensuring correct operation in any working condition, sliding mode controller is one of the most feasible approach offered.

Sliding mode control has been presented as a good alternative to the control of switching power converters [3] - [8]. The main advantage over the classical control schemes is its robustness for plant parameter variation, that leads to invariant dynamics and steady state response in the ideal case.

In this paper a sliding mode controller for the boost inverter is proposed. Details on analysis, simulation and experimentation are presented in the subsequent sections.

SYSTEM DESCRIPTION

In Fig. 1 it is shown the boost DC to AC converter. The power stage is configured on the current bi-directional boost converter. It includes: dc supply voltage V_{in} , input inductors L_1 and L_2 , power switches $S_1 - S_4$, transfer capacitors C_1 and C_2 , free - wheeling diodes $D_1 - D_4$ and load resistance R_L .

The main purpose of the controllers A and B is the following: the outputs (capacitor voltage V_1 and V_2) must follow a sinusoidal reference, the most faithfully as possible.

The boost inverter achieves DC - AC conversion as follows: this boost inverter is arranged by two bi-directional boost converter. These converters produce a DC - biased sine wave output, so that each converter only produces an unipolar voltage. The modulation of each converter is 180 degrees out of phase with the other, which maximizes the voltage excursion over the load. The load is connected differentially across the converter. Thus, whereas a DC bias appears at each end of the load with respect to ground, the differential DC voltage over the load is zero.

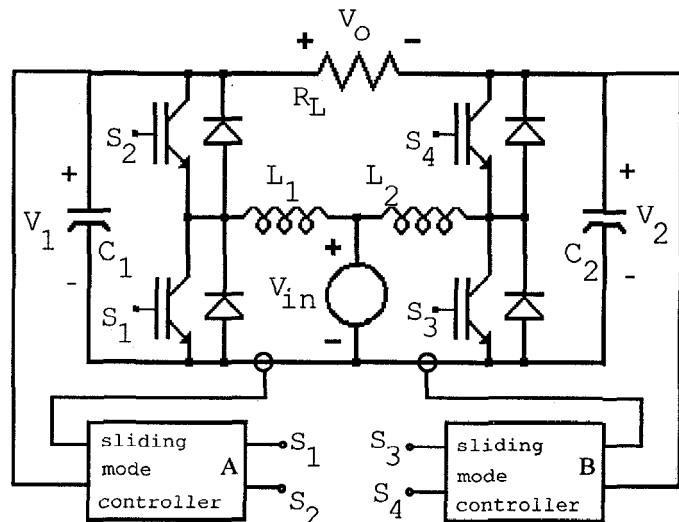


Fig. 1 The boost inverter controlled by sliding mode.

The operation of the boost inverter is better understood through the current bi-directional boost converter shown in Fig. 2.

In the description of the operation of the converter, it is assumed that all the components are ideal and the converter operates in continuous conduction mode. Fig. 3 shows two (2) topological modes, for a period of operation.

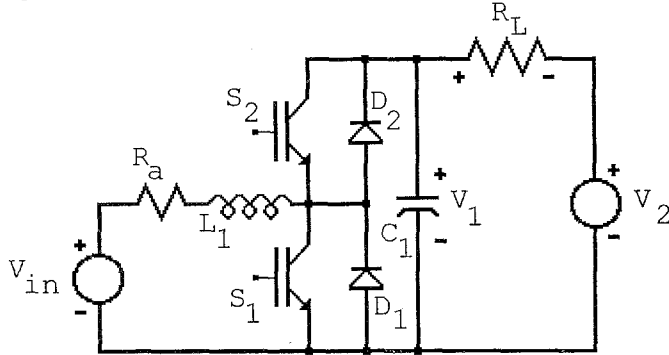


Fig. 2 Equivalent circuit for the boost inverter.

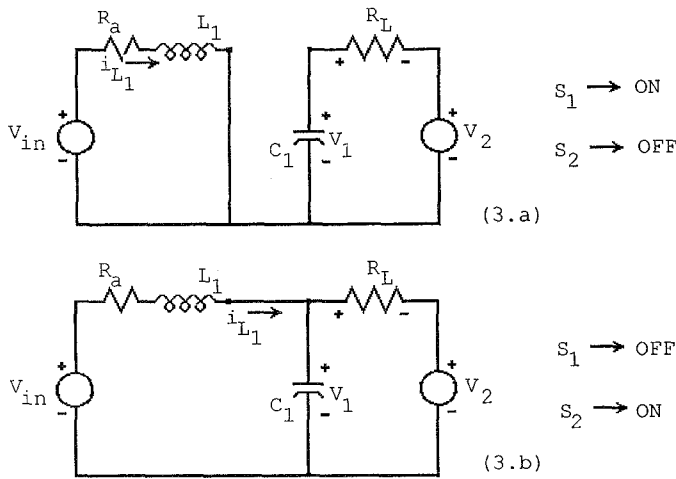


Fig. 3 Modes of Operation.

When the switch S_1 is closed and S_2 is open (Fig. 3.a) current i_{L1} rises quite linearly, diode D_2 is reverse biased and capacitor C_1 supplies energy to the output stage, decreasing voltage V_1 .

Once the switch S_1 is open and S_2 is closed (Fig. 3.b) current i_{L1} flow through capacitor C_1 and the output stage. The current i_{L1} decreases while capacitor C_1 is recharged.

The state space modeling of the equivalent circuit with state variables i_{L1} and V_1 , gives:

$$\begin{bmatrix} \frac{di_{L1}}{dt} \\ \frac{dV_1}{dt} \end{bmatrix} = \begin{bmatrix} \frac{-R_a}{L_1} & \frac{-1}{L_1} \\ \frac{1}{C_1} & \frac{-1}{L_1} \end{bmatrix} \begin{bmatrix} i_{L1} \\ V_1 \end{bmatrix} + \begin{bmatrix} \frac{V_1}{L_1} \\ \frac{-i_{L1}}{C_1} \end{bmatrix} \gamma + \begin{bmatrix} \frac{V_{in}}{L_1} \\ \frac{V_2}{C_1 R_L} \end{bmatrix} \quad (1)$$

$$\mathbf{v} = \mathbf{A} \mathbf{v} + \mathbf{B} \gamma + \mathbf{C}$$

where γ is the switches status, \mathbf{v} and \mathbf{v} are the vectors of the status variables (i_{L1} , V_1) and their time derivatives, respectively.

$$\gamma = \begin{cases} \mathbf{1} & \rightarrow S_1 \text{ ON, } S_2 \text{ OFF} \\ \mathbf{0} & \rightarrow S_1 \text{ OFF, } S_2 \text{ ON} \end{cases} \quad (2)$$

SLIDING - MODE CONTROLLER

When good transient response of the output voltage is needed, a sliding surface $S(i_{L1}, V_1)$ can be chosen to be [6]:

$$S(i_{L1}, V_1) = K_1 \epsilon_1 + K_2 \epsilon_2 = 0 \quad (3)$$

The sliding surface equation $S(i_{L1}, V_1)$, in the state space, is expressed by a linear combination of state variable errors ϵ_i . Where, ϵ_1 is the feedback current error and ϵ_2 is the feedback voltage error, or:

$$\epsilon_1 = i_{L1} - i_{Lref} \quad (4) \quad \epsilon_2 = V_1 - V_{ref} \quad (5)$$

substituting (4) and (5) in (3), it is obtained:

$$S(i_{L1}, V_1) = K_1(i_{L1} - i_{Lref}) + K_2(V_1 - V_{ref}) \quad (6)$$

The signal $S(i_{L1}, V_1)$, obtained by the hardware implementation of equation (6), and applied to a simple circuit (hysteresis comparator), can generate the pulses to supply the power semiconductor drives.

The corresponding control scheme is shown in Fig. 4. Switch status γ is controlled by hysteresis block H1 so that variable $S(i_{L1}, V_1)$ is maintained near zero.

The system response is determined by the circuit parameters and coefficients (K_1 , K_2). With a proper selection of these coefficients, high control robustness, stable and fast response can be achieved, for any operating condition.

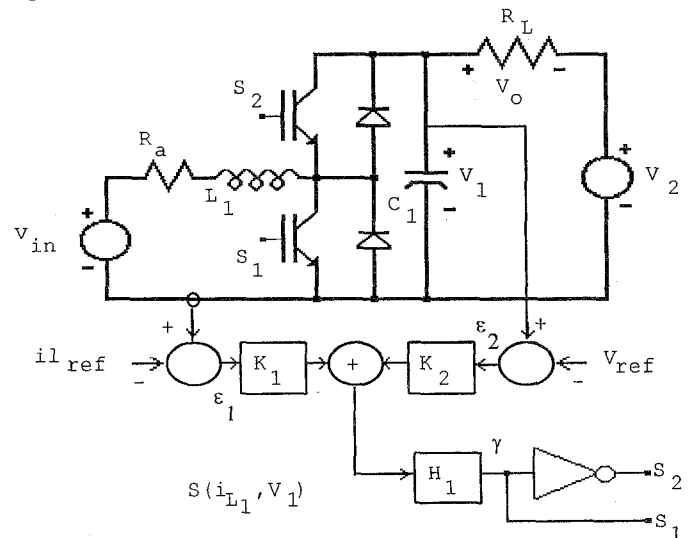


Fig. 4 Sliding mode controller scheme.

In practice, the reference signal i_{Lref} is actually not required, since steady state values of variable i_{L1} automatically adapt to actual converter operation. Thus, only the high frequency component of this variable is needed for the control, and error signal ($i_{L1} - i_{Lref}$) can be obtained, from feedback variable i_{L1} , by means of a high pass filter.

Selection of control parameters

Once the boost inverter parameters were selected, inductances L_1 and L_2 are designed from specified input and output current ripples; capacitors C_1 and C_2 are designed to limit the output voltage ripple in the case of fast and large load variations; maximum switching frequency is selected from the converter ratings and switch type. The system behaviour is completely determined by coefficients (K_1, K_2), which must be selected in order to satisfy existence, ensure stability and fast response, even for large supply and load variations.

According to the variable structure system theory, the converter equations must be written in the following form:

$$\dot{\mathbf{x}} = \mathbf{Ax} + \mathbf{By} + \mathbf{D} \quad (7)$$

where \mathbf{x} represents the vector of state variables errors, given by:

$$\mathbf{x} = \mathbf{v} - \mathbf{V}^* \quad (8)$$

where $\mathbf{V}^* = [i_{Lref}, V_{ref}]^T$ is the vector of references (index T means transposition).

Substituting (8) in (1) it is obtained:

$$\mathbf{D} = \mathbf{AV}^* + \mathbf{C} \quad (9)$$

$$\mathbf{D} = \begin{bmatrix} \frac{-R_a}{L_1} & \frac{-1}{L_1} \\ \frac{1}{L_1} & \frac{-1}{C_1 R_L} \end{bmatrix} \begin{bmatrix} i_{Lref} \\ V_{ref} \end{bmatrix} + \begin{bmatrix} \frac{V_{in}}{L_1} \\ \frac{V_2}{C_1 R_L} \end{bmatrix} \quad (10.a)$$

$$\mathbf{D} = \begin{bmatrix} -\frac{V_{ref}}{L_1} + \frac{V_{in}}{L_1} - \frac{R_a i_{Lref}}{L_1} \\ -\frac{V_{ref}}{C_1 R_L} + \frac{V_2}{C_1 R_L} + \frac{i_{Lref}}{C_1} \end{bmatrix} \quad (10.b)$$

Substituting (8) in (6), the sliding function can be rewritten in the form:

$$\mathbf{S}(\mathbf{x}) = \mathbf{K}_1 \mathbf{x}_1 + \mathbf{K}_2 \mathbf{x}_2 = \mathbf{K}^T \mathbf{x} \quad (11)$$

The existence condition of the sliding mode requires that all state trajectories, near the surface, are directed toward the sliding plane. The controller can enforce the

system state to remain near the sliding plane by proper operation of the converter switches.

To make the system state move towards the switching surface, it is necessary and sufficient that:

$$\begin{cases} \dot{\mathbf{S}} < 0 & \text{if } \mathbf{S} > 0 \\ \dot{\mathbf{S}} > 0 & \text{if } \mathbf{S} < 0 \end{cases} \quad (12)$$

Sliding mode control is obtained by means of the following feedback control strategy, which relates the switches status with the value of $\mathbf{S}(\mathbf{x})$:

$$\gamma = \begin{cases} 0 & \text{for } \mathbf{S}(\mathbf{x}) > 0 \\ 1 & \text{for } \mathbf{S}(\mathbf{x}) < 0 \end{cases} \quad (13)$$

The existence condition (12) can be expressed in the form:

$$\dot{\mathbf{S}}(\mathbf{x}) = \mathbf{K}^T \mathbf{Ax} + \mathbf{K}^T \mathbf{D} < 0; \quad 0 < \mathbf{S}(\mathbf{x}) < \delta \quad (14)$$

$$\dot{\mathbf{S}}(\mathbf{x}) = \mathbf{K}^T \mathbf{Ax} + \mathbf{K}^T \mathbf{B} + \mathbf{K}^T \mathbf{D} > 0; \quad -\delta < \mathbf{S}(\mathbf{x}) < 0 \quad (15)$$

where δ is an arbitrarily small positive quantity.

From a practical point of view, the assumption that error variables x_i are suitably smaller than references V^* , the equations (14) and (15) can be rewritten in the form:

$$\mathbf{K}^T \mathbf{D} < 0 \quad 0 < \mathbf{S}(\mathbf{x}) < \delta \quad (16)$$

$$\mathbf{K}^T \mathbf{B} + \mathbf{K}^T \mathbf{D} > 0 \quad -\delta < \mathbf{S}(\mathbf{x}) < 0 \quad (17)$$

Substituting matrices \mathbf{B} and \mathbf{D} in (16) and (17), it is obtained:

$$\frac{K_1}{L_1} [V_{in} - V_{ref} - R_a i_{Lref}] + \frac{K_2}{C_1 R_L} [V_2 - V_{ref} + R_L i_{Lref}] < 0 \quad (18)$$

$$\frac{K_1}{L_1} [V_{in} - R_a i_{Lref}] + \frac{K_2}{C_1 R_L} [V_2 - V_{ref}] > 0 \quad (19)$$

The existence condition is satisfied if the inequalities (18) and (19) are true.

In the ideal sliding mode, at infinite switching frequency, state trajectories are directed towards the sliding surface and move exactly along the surface. Practical system can not switch at infinite frequency, so a typical control circuit features an hysteresis comparator with width 2δ , the switching occurs at $|\mathbf{S}(\mathbf{x})| > \delta$ with a frequency depending on the slopes of i_{L1} . This hysteresis causes phase plane trajectory oscillations of width 2δ , around the surface $\mathbf{S}(\mathbf{x})=0$.

The constant hysteresis implies variable frequency, non periodic action. Therefore, sliding mode control is not well adapted for driving system requiring fixed frequency operation.

Simulation Results

The boost DC - AC converter, in Fig. 1, was simulated using a computer simulation program, assuming: ideal power switches, ideal output capacitor and power supply voltage and inductors with internal resistance R_a . The following parameters were adopted in these simulation:

$$V_{in} = 100 \text{ V}$$

$$V_o = 180 \sin(2\pi 60 \text{ Hz})t$$

$$P_o = 500 \text{ W}$$

$$R_L = 30 \Omega$$

$$L_1, L_2 = 750 \mu\text{H each.}$$

$$C_1, C_2 = 20 \mu\text{F each}$$

$$f_{s_{max}} = 30 \text{ kHz}$$

The parameters of the controller are as follows:

$$K_1 = 0.197, K_2 = 0.020 \text{ and } \delta = 0.3$$

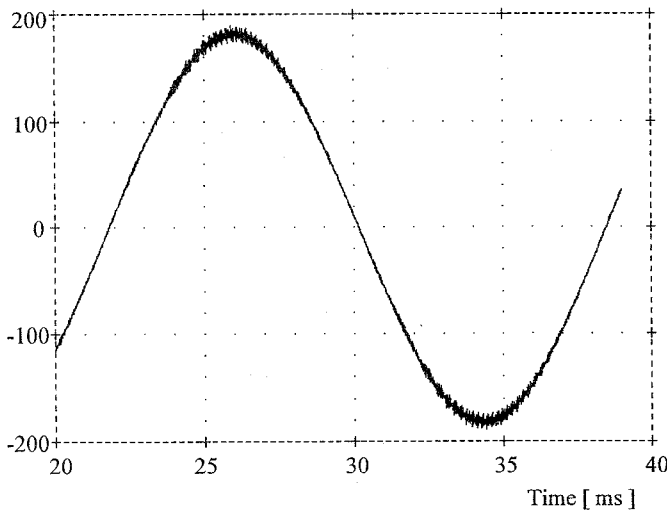


Fig. 5 Output voltage V_o .

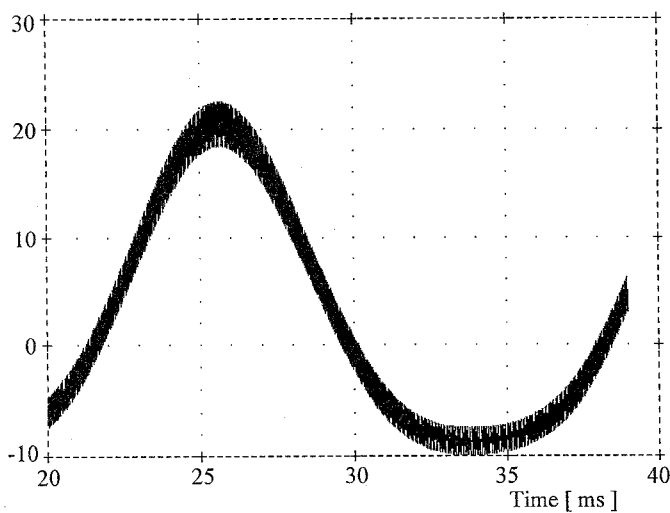


Fig. 6 Current of the inductor L_1 .

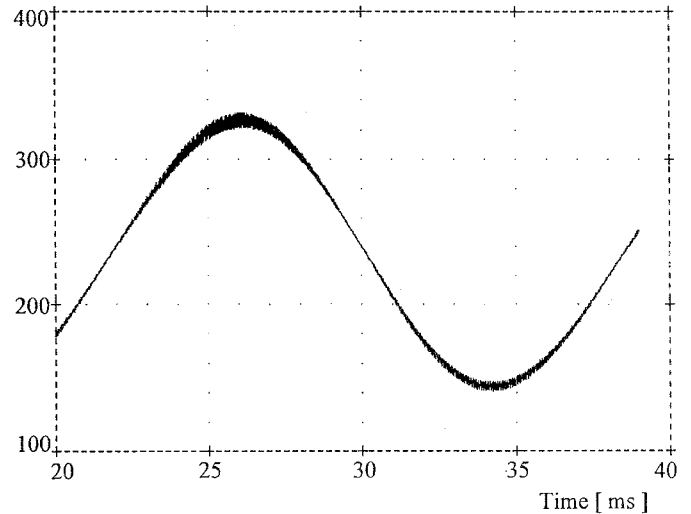


Fig. 7 Voltage of the capacitor C_1 .

Fig. 5, 6 and 7 show simulated waveforms of the converter for a resistive load of 500 W.

Fig. 5 shows the inverter output voltage. The instantaneous AC voltage is 170 V, which means a r.m.s value equal to 120 V. The total harmonic distortion is lower than 0.3 %.

In Fig. 6 it is showed the inductor current i_{L1} . The maximum inductor current is 22 A, the maximum current ripple is 4 A, when V_1 is maximum.

Fig. 7 shows the capacitor voltage V_1 . The maximum capacitor voltage is 330 V and the minimum voltage is 140 V. The maximum voltage ripple is 10 V, when V_1 is maximum.

Experimental Results

In order to confirm the effective performance, key experiments were implemented with a 500W prototype of the proposed converter shown in Fig. 1.

The parameter of the circuits are as follows:

S1 - S4: IRGBC20U (IGBT)

D1 - D4: MUR850 (Diodes)

C1, C2: 20 μF / 600 V each

L1, L2: 750 μH each

Input and output specifications are:

Input V_{in} : 100 V

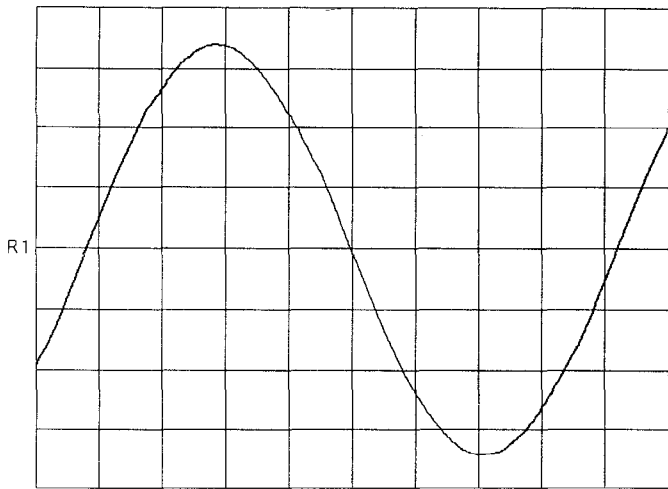
output V_o : $180 \cdot \sin(2\pi \cdot 60\text{Hz}) \cdot t$

$f_{s_{max}}$: 30 kHz

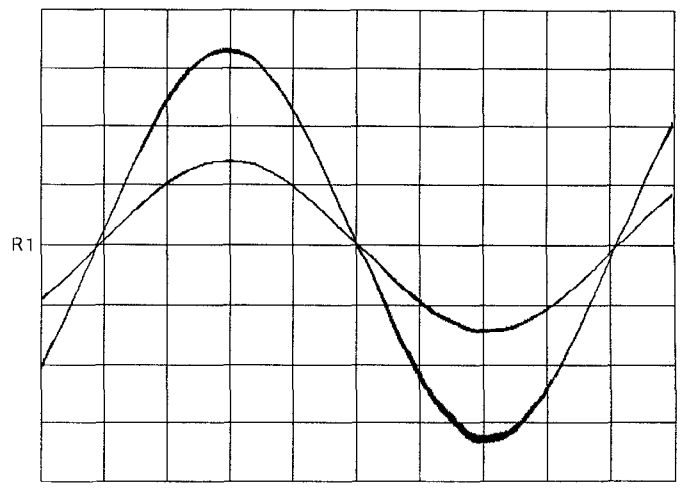
The parameters of the controller are:

$K_1 = 0.197, K_2 = 0.020$ and $\delta = 0.3$

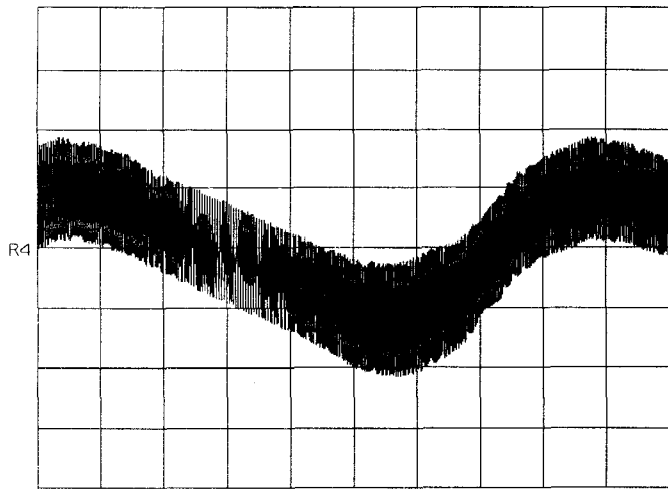
The operation at no load is presented in Fig. 8, 9 and 10. The inverter output voltage is shown in Fig. 8. The total harmonic distortion is 1.16 %. In Fig. 9 it is shown the inductor current i_{L1} . Fig. 10 shows the capacitor voltage.



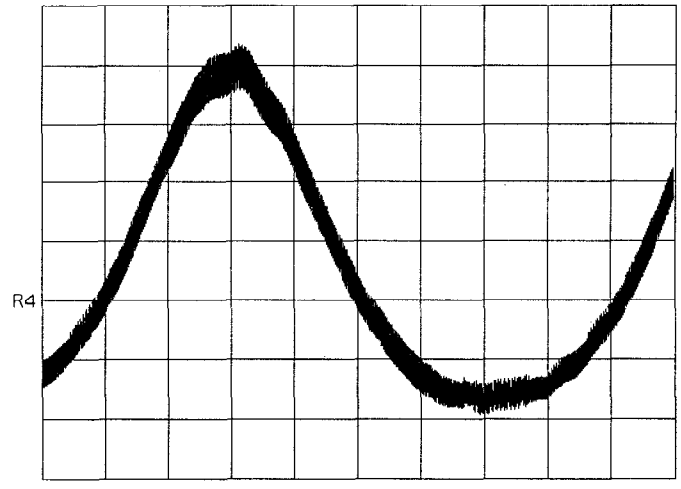
Ref1 50.0 V 2.00ms
Fig. 8 Output voltage, unload inverter.



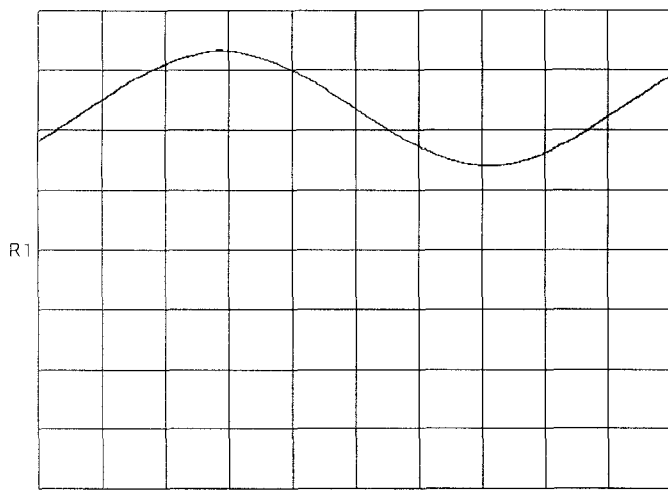
50 V 4.00 A 2.00 ms
Fig. 11 Resistive load operation, $P_o = 497$ W.



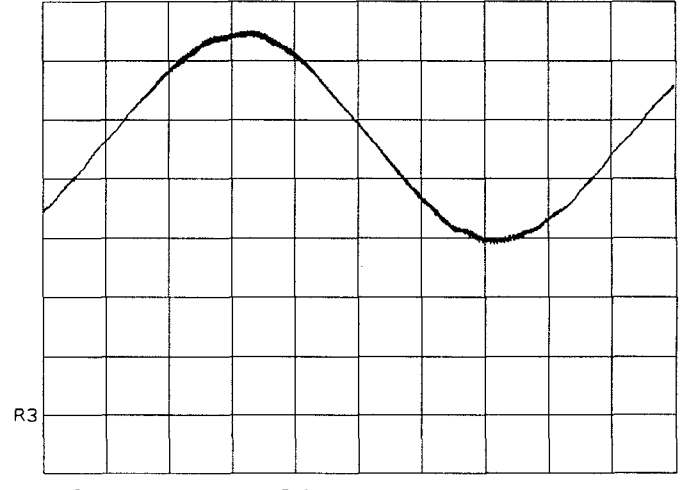
Ref4 2 A 2.00ms
Fig. 9 Current of the inductor L_1 , unload inverter.



Ref4 5.0 A 2.00 ms
Fig. 12 Current of the inductor L_1 , $P_o = 497$ W.



Ref1 100 V 2.00ms
Fig. 10 Voltage of the capacitor C_1 , unload inverter.



Ref3 50.0 V 2.00ms
Fig. 13 Voltage of the capacitor C_1 , $P_o = 497$ W.

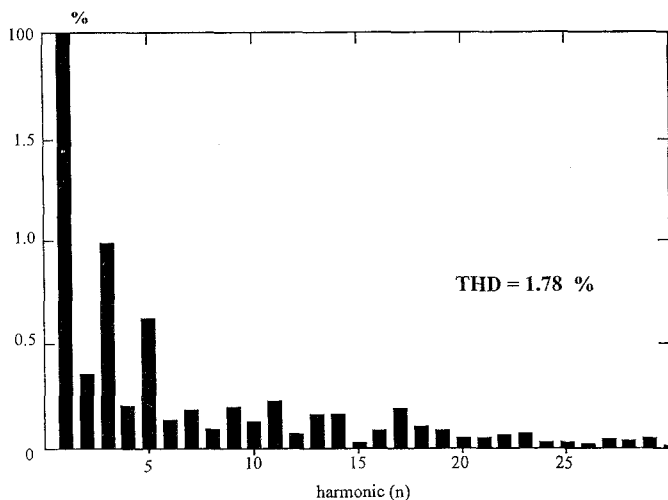


Fig. 14 Output voltage harmonic analysis of the inverter operating with resistive load, $P_o = 497$ W.

Fig. 11, 12 and 13 show experimental waveforms of the converter for resistive load of 500 W, $R_L = 30 \Omega$. The experimental results are in good agreement with the simulation results.

The Fig. 11 shows the inverter output current and output voltage. The output rms current is 4.14 A, the output rms voltage is 120 V, which means that the output power is 497 W. In Fig. 12 it is shown the inductor current i_{L1} . Fig. 13 shows the capacitor voltage V_{C1} .

The fig. 14 shows harmonic analysis of inverter output voltage with resistive load, $P_o = 497$ W. The total harmonic distortion is 1.78 %, and the third harmonic is the greatest, with 1 %.

CONCLUSION

A sliding mode controller applied to the DC - AC boost converter achieved stability with respect to load parameter variation and good static behaviour. The controller has a fast dynamic response, since all control loops act concurrently, and the robustness inherent to sliding mode control.

In this case, the boost inverter operate with variable frequency, switching frequency varies depending on the working point.

By means of this controller, the converter generates a sinusoidal output voltage with a total harmonic distortion lower than 2%.

The circuit operation has been described and discussed. The performance are verified experimentally on a 500 W breadboard. The simulation and experimental results validate the proposed control strategy and the sliding surface.

References

- [1] R. Caceres and Ivo Barbi, "A boost DC - AC Converter: Operation, Analysis, Control and Experimentation", Proceedings of International Conference on Industrial Electronics, Control and Instrumentation (IECON'95), Orlando, USA, Nov 6 - 10, 1995. pp 546 - 551.
- [2] R. Caceres and Ivo Barbi, "A boost DC - AC Converter: Design, Simulation and Implementation", Proceedings of the Power Electronic Brazilian Congress (COBEP'95), São Paulo, Brazil, Dec 4 - 7 1995.
- [3] H. Sira-Ramirez, "Sliding Mode Control of AC to AC Converters", Proc. Brazilian Congress of Automatic (CBA'88), pp 452 - 457.
- [4] M. Rios-Bolivar and H. Sira-Ramirez "An Extended Linearization approach to Sliding Mode Control of DC to DC Power Supplies", Proc. COBEP 1991, pp 21 - 26.
- [5] M. Carpita, P. Farina, S. Tenconi "A single phase, Sliding Mode Controlled Inverter with three levels output voltage for UPS or Power Conditioning Applications" Proc. EPE 1993, pp 272 - 277.
- [6] L. Malesani, L. Rossetto, G. Spiazzi, P. Tenti "Performance Optimization of Cuk Converter by Sliding Mode Control", Proc. APEC 1992, pp 395 - 402.
- [7] P. Mattavelli, L. Rossetto, G. Spiazzi "General Purpose Sliding Mode Controller for DC - DC converter Applications", Proc. PESC 1993, pp 609 - 615.
- [8] H. Pinheiro, A.S. Martins, J.R. Pinheiro "Monophasic Voltage Inverters controlled by Sliding Mode" (in Portuguese), Proc. CBA 1994, pp 1177 - 1182.